Power System Technology
ISSN:1000-3673

Received: 16-06-2025 *Revised: 05-07-2025* *Accepted: 20-08-2025*

Improved Soft Switching Technique for Dual Active Bridge Converter Applied to Electric Vehicle Fast Charging System

Anbuselvi SV, Brinda R, Pradhip Raj T, Kumudini Devi RP

Department of Electrical and Electronics Engineeering, College of Engineering Guindy, Anna University, Chennai, India

Abstract:-The Electric Vehicle Fast Charging System (EVFCS) consists of an AC-DC converter and multiple DC-DC converters to charge the Electric Vehicle (EV) battery. The Dual Active Bridge (DAB) Converter is the most promising topology of DC-DC converter owing to its advantages such as galvanic isolation, bidirectional capability, high voltage gain, inherent soft switching and high efficiency. The DAB converter controls are designed to achieve Constant Current (CC) Charging. It is controlled by employing Phase Shift Modulation (PSM) techniques to achieve the desired power transfer. The Voltage Source Converter (VSC), is the front end AC-DC converter which is designed to maintain a stiff DC bus voltage. In this work, the DAB converter is controlled by employing improved Triple Phase Shift (TPS) scheme to improve the soft switching region for the converter. The proposed control scheme is verified with the simulations performed in MATLAB/Simulink and the experimental validations are done using Real Time Digital Simulator OP4610.

Keywords*: Dual Active Bridge Converter, DC Fast Charging, Electric Vehicle, VSC, Triple Phase Shift.*

Nomenclature:

DAB – Dual Active Bridge
DPS – Dual Phase Shift
EPS – Extended Phase Shift
EV – Electric Vehicle
EVFCS – Electric Vehicle Fast Charging System
G2V – Grid to Vehicle
PFC – Power Factor Correction
PI – Proportional Integral
SPS – Single Phase Shift
TPS – Triple Phase Shift
V2G- Vehicle to Grid
VSC – Voltage Source Converter
ZCS – Zero Current Switching
ZVS – Zero Voltage Switching

Power System Technology
ISSN:1000-3673

Received: 16-06-2025 *Revised: 05-07-2025* *Accepted: 20-08-2025*

1. Introduction

With the increasing concern about the negative impacts of the transportation sector on the environment, research on sustainable transportation has increased. Electric Vehicles (EVs) are getting more attraction in the transportation sector as an alternative to conventional fossil fuel vehicles due to the rising awareness of carbon emission [1]. The shift towards EVs necessitates the development of highly efficient charging infrastructure. The EV batteries are powered from the utility grid by means of power converters. The Electric Vehicle Charging System is a key component in the adoption of EV for transportation [2]. The EV chargers are of two types based on the type of charging – AC charging and DC charging. AC chargers are of level 1 and level 2 which are onboard chargers. The DC chargers are of level 3 which are off-board chargers [3]. The EV charging can be either two stage conversion or single stage conversion. The single stage EV charger has a converter that performs the Power Factor Correction (PFC) as well as regulates the battery charging current. The two stage EV charger comprises of an AC-DC converter at the first stage which performs PFC and at the second stage, a DC-DC converter which is designed to control the charging current. Two stage EV charging is preferred over the single stage charging since the converter topologies are simpler, control strategy is simpler, and has better dynamic performance [4-9].

The level 3 off-board charger comprises of AC-DC converter and DC-DC converter which are located outside. The AC-DC converter is the first stage of power conversion in the EVCS which is connected to the AC grid of 415V [10]. The primary objective of the AC-DC conversion stage is to ensure a stiff DC bus voltage of 800V. The other objectives of the first stage conversion are Power Factor Correction (PFC) and Harmonic Elimination. The DC-DC converter is at the second stage of power conversion. The objectives of the DC-DC stage are regulation of output voltage and output current.

In the literature various topologies of AC-DC converters such as three-phase buck rectifier, Swiss rectifier, Vienna rectifier, three-phase boost type rectifier and multilevel AC-DC topologies are used for DC Fast Charging applications. In this work, three-phase boost rectifier is used due to its simple topology, lesser components, bidirectional operation, high output DC voltage, low current stress, simple control structure, low THD and high efficiency.

Various topologies of bidirectional DC-DC Converters used in DC Fast Charger are discussed in the literature. The isolated DC-DC converters are preferred over the non-isolated converters since the DC-DC power converter is connected to the battery and isolation becomes essential during high power operation. The Dual Active Bridge (DAB) Converter is one of the most attractive DC-DC converter for EV charging applications due to its bidirectional capability, high power density, high power handling capability, reduced component count and inherent ZVS capability. The DAB converter proposed by

Power System Technology
ISSN:1000-3673
Received: 16-06-2025 Revised: 05-07-2025 Accepted: 20-08-2025

Kheraluwala, et al [11] for high power DC-DC conversion is widely used in SST (Solid State Transformer), DC microgrid, Energy storage, Electric Vehicle and renewable energy applications. The basic DAB converter topology consists of two H-bridges connected by a high frequency transformer with a series inductor which acts as the energy transfer element. Another advantage of DAB converter is its modularity, which allows scaling to higher power level.

The control objectives of AC-DC power conversion stage are DC bus voltage regulation and power factor correction. The cascaded Proportional Integral control based on dq transformation is used to control the AC-DC converter. DC voltage regulation is achieved by outer voltage loop and reactive power is controlled by outer reactive power loop.

The power transfer in the DAB converter is described by the relation [12]

$$P = \frac{N\, V_i V_o d\, (1-d)}{2 f_s\ L} \qquad (1)$$

Where d is the phase shift ratio between the two bridges

f_s is the switching frequency of the converter

L is the equivalent inductance

N is the turns ratio of the high frequency transformer

V_i is the DC bus voltage

V_o is the output voltage of the DAB converter

From (1) it can be observed that the power transfer in the DAB converter can be regulated by controlling the phase shift between the two bridges. In the literature, the DAB converter is controlled by various modulation techniques such as Single Phase Shift (SPS), Extended Phase Shift (EPS), Dual Phase Shift (DPS), Triple Phase Shift (TPS) and frequency modulation techniques [12]. SPS modulation is the simplest and hence most commonly used technique for achieving power transfer in the DAB converter. With SPS scheme, the efficiency of DAB at various operating conditions get comprised since the scheme offers single degree of freedom. Achieving wide range ZVS with SPS is not possible and hence other advanced modulation schemes such as EPS, DPS, TPS are preferred to control the converter. EPS controls phase shift between the two legs (inner phase shift) of the primary bridge in addition with the phase shift between the two bridges. EPS also has limited effectiveness at light loads, and has reactive power circulation. DPS controls power transfer by controlling the inner phase shift of both the bridges and the outer phase shift. The ZVS range in the converter is increased with the introduction of inner phase shift. Optimization

Power System Technology
ISSN:1000-3673
Received: 16-06-2025 Revised: 05-07-2025 Accepted: 20-08-2025

along with DPS is discussed in [13] which minimizes the reactive power in the converter at light loading conditions. The major drawback of DPS scheme is that since the inner phase shift of both the bridges are identical, the converter cannot operate with high efficiency in all operating zones. In [9] TPS modulation strategy has been introduced to overcome the drawbacks of DPS. With TPS three degrees of freedom are achieved. With TPS control, the conduction loss is reduced, wide range of ZVS is achieved, the peak inductor current is minimized and the reactive power is reduced. In this work improved TPS modulation scheme is proposed to improve the soft switching range of the DAB converter.

The subsequent sections of the paper are organized as follows: the system configuration of the DAB based EVFCS is described in section 2. In section 3, the operation of the EVFCS and the various control strategies are discussed. In section 4, the dynamic model of the EVFCS is presented. Detailed simulation results obtained with MATLAB/Simulink is presented in section 5. In the section 6, the experimental validation of the EVFCS with the proposed control is discussed along with the experimental results. Finally, section 7 provides the conclusion of the contributions from the work.

2. System Configuration of the EVFCS

The block diagram of the EVFCS is shown in fig 1. It consists of a three phase two level Voltage Source Converter (VSC) connected to the AC grid and two number of DAB converters connected to the common DC bus. The output of the DAB is connected to the battery. The VSC maintains a stiff DC bus voltage of 800V and is controlled by employing independent dq control. The VSC is connected to the AC grid by means of LCL filter and converter transformer. The design of the LCL filter was carried out along the lines of [14].

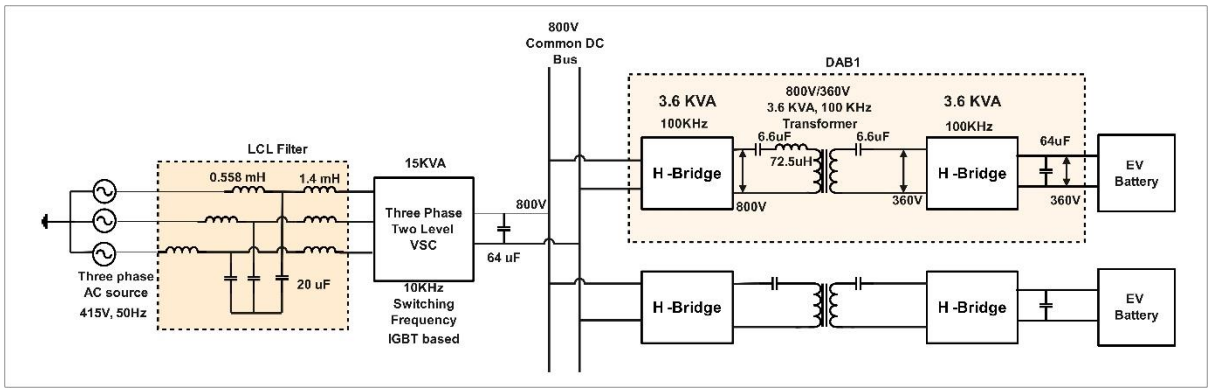

Figure 1: Block diagram of the off-board EVFCS

The DAB converter consists of two H-bridges, denoted as HB1 and HB2, connected through a High Frequency (HF) transformer of turns ratio n and a CLC resonant tank circuit. The

Power System Technology
ISSN:1000-3673
Received: 16-06-2025 Revised: 05-07-2025 Accepted: 20-08-2025

selection of turns ratio n, of the HF transformer depends upon the voltage of the common DC bus and the output voltage requirement of the DAB converter. The output of the DAB converter is connected to the EV battery stack.

3. Operation and Control of EVFCS

The VSC is controlled by employing independent dq control. The objectives of the VSC controllers are DC bus voltage regulation and reactive power control. The reference voltages thus obtained from the controllers are used to generate the firing pulses to the IGBT switches of VSC by Sinusoidal Pulse Width Modulation (SPWM). The controllers of the VSC are tuned by using small signal stability analysis to ensure closed loop stability with the cascaded controllers [15]. The gain parameters of the controllers thus obtained from the small signal stability based tuning are used in the simulation.

The control strategy that is most fundamental in DAB converter is the Phase Shift Modulation (PSM) control which involves the control of phase shift between the two H-bridges to regulate the power transfer. The PSM techniques that are used to regulate the power transfer in DAB converter are Single Phase Shift (SPS), Extended Phase Shift (EPS), Dual Phase Shift (DPS) and Triple Phase Shift (TPS). With SPS control the outer phase shift (d) between the two H-bridges is controlled to regulate the power transfer. In EPS, the inner phase shift (d1) within the first H-bridge and the outer phase shift (d) are controlled to regulate the active power transfer. With DPS control, the inner phase shift (d1) within each H-bridge and the outer phase shift (d) are controlled. With TPS control the inner phase shifts (d1 and d2) within each H-bridge and the outer phase shift (d) are controlled.

The detailed control structure of the EVFCS is shown in fig 2. The VSC is connected to the AC grid through converter transformer and LCL filter. The LCL filter is designed to mitigate the harmonics penetrating into the grid. The VSC is three legged IGBT based boost recitifer type AC-DC Converter. The front end VSC is controlled by employing SPWM technique where the reference signals are obtained from the independent vector control. The voltage at the point of common coupling is sensed and the angle is extracted with the PLL required for the transformations. The q axis current reference for the inner current controller of VSC is set to zero so as to achieve minimum reactive power operation. The DAB converter is connected to the DC bus of VSC and it is controlled by improved TPS control where the phase shifts (d) and (d1, d2) are obtained from the PI controllers which ensure soft switching in the entire range of operation. The inner phase shifts are obtained from the PI controller whose objective is to minimise the reactive power consumed by the high frequency transformer. The high frequency transformer connected between the two H-bridges of the DAB provide isolation and is chosen based on the voltage requirements. The high frequency transformer is made of ferrite core to operate at high frequencies of the order of 100 kHz. The switching scheme is

Power System Technology
ISSN:1000-3673
Received: 16-06-2025 Revised: 05-07-2025 Accepted: 20-08-2025

realised with the cascaded PI controllers which are tuned to achieve soft switching in the entire range of operation.

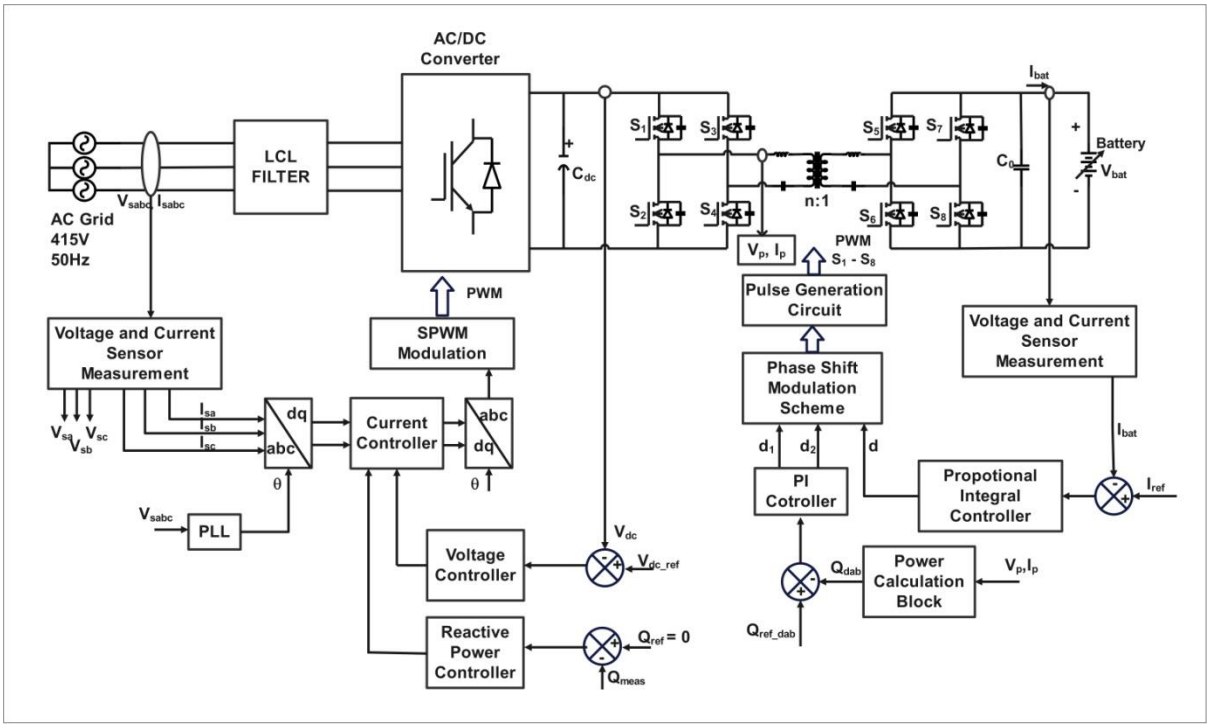

Figure 2: Detailed Control Structure of the EVFCS

4. Dynamic Modeling of EVFCS

The VSC is controlled with conventional grid voltage vector orientation control with q axis leading the d axis and the voltage at the point of common coupling is aligned with the d-axis [15]. The dynamic model of the VSC is given by

Modelling of the AC and DC system:

$$V_s^{\,d} - V_c^{\,d} = R\, i_c^{\,d} - \omega . L . i_c^{\,q} + L \frac{d i_c^{\,d}}{dt} \tag{2}$$

$$V_s^{\,q} - V_c^{\,q} = R\, i_c^{\,q} - \omega . L . i_c^{\,d} + L \frac{d i_c^{\,q}}{dt} \tag{3}$$

$$C_{DC} . \frac{dV_{dc}}{dt} = i_{DC} - i_{DAB} \tag{4}$$

Modelling of the DC Voltage Controller:

$$i_{dc_{ref}} = [K_{p_{dc}} + \frac{Ki_{dc}}{S}](V_{dc_{ref}} - V_{dc}) \tag{5}$$

$$\dot{N_{dc}} = K_{i_{dc}}(V_{dc_{ref}} - V_{dc}) \tag{6}$$

Power System Technology
ISSN:1000-3673
Received: 16-06-2025 Revised: 05-07-2025 Accepted: 20-08-2025

$$\dot{i}_{dc_{ref}}\left(\frac{1}{1+sT_{dc}}\right) = i_{dc} \quad (7)$$

Modelling of the inner current controllers:

$$V_{c_{ref}}^{\dot{d}} = (i_{c_{ref}}^{d} - i_{c}^{d})[K_{p_{fd}} + \frac{Ki_{fd}}{S}] - \omega.L.i_{c}{}^{q} + V_{s}^{d} \quad (8)$$

$$\dot{M_{dc}} = \left(i_{c_{ref}}^{d} - i_{c}^{d}\right) K_{i_{fd}} \quad (9)$$

$$V_{c}^{d} = \left(\frac{1}{1+ST}\right) V_{c_{ref}}^{d} \quad (10)$$

$$\left(V_{s_{ref}}^{d} - v_{s}^{d}\right)\left(K_{p_{ac}} + \frac{K_{i_{ac}}}{s}\right) = i_{c_{ref}}^{q} \quad (11)$$

$$\Delta i_{c_{ref}}^{q} = \left(V_{s_{ref}}^{d} - v_{s}^{d}\right).K_{p_{ac}} + \Delta N_{ac} \quad (12)$$

$$\dot{N_{ac}} = -K_{i_{ac}}\left(V_{s_{ref}}^{d} - v_{s}^{d}\right) \quad (13)$$

$$\left(i_{c_{ref}}^{q} - i_{c}^{q}\right)\left[K_{p_{fq}} + \frac{K_{i_{fq}}}{s}\right] + \omega L i_{c}^{d} = V_{c_{ref}}^{q} \quad (14)$$

$$\dot{M_{ac}} = K_{i_{fq}}(i_{c_{ref}}^{q} - i_{c}^{q}) \quad (15)$$

$$\dot{\Delta M_{ac}} = K_{i_{fq}}\left(\left(V_{s_{ref}}^{d} - v_{s}^{d}\right).K_{p_{ac}} + \Delta N_{ac}\right) - K_{i_{fq}} i_{c}^{q} \quad (16)$$

$$V_{c}^{q} = \left(\frac{1}{1+sT}\right) V_{c_{ref}}^{q} \quad (17)$$

$$V_{c}^{q} + V_{c}^{q}.sT = V_{c_{ref}}^{q} \quad (18)$$

$$\dot{V_{c}^{q}} = \frac{1}{T}\left[V_{c_{ref}}^{q} - v_{c}^{q}\right] \quad (19)$$

The dynamic equations of DAB Converter obtained by Generalized Averaging Method [16] are given by (20 – 22)

The equations for transformer current and output voltage of DAB after considering the zeroth component for DC and real and imaginary component for transformer current (AC), the final dot equations are,

Power System Technology
ISSN:1000-3673

Received: 16-06-2025 Revised: 05-07-2025 Accepted: 20-08-2025

$$\frac{d\langle i_t\rangle_{1R}}{dt} = -\frac{R_t}{L_t}\langle i_t\rangle_{1R} + w_S\langle it\rangle_{1I} + \frac{1}{L_t}(\langle s_1\rangle_0\langle v_i\rangle_{1R} + \langle s_1\rangle_{1R}\langle v_i\rangle_0) - \frac{1}{L_t}(\langle s_2\rangle_0\langle v_0\rangle_{1R} + \langle s_2\rangle_{1R}\langle v_0\rangle_0 = -\frac{R_t}{L_t}(it_{1R}) - w_S(it_{1I}) + \frac{1}{L_t}\frac{-2\sin d\pi}{\pi}(v_i) - \frac{1}{L_t}\frac{-2\cos d\pi}{\pi}(v) \quad (20)$$

$$\frac{d\langle i_t\rangle_{1I}}{dt} = -\frac{R_t}{L_t}\langle i_t\rangle_{1I} - w_S\langle it\rangle_{1R} + \frac{1}{L_t}(\langle s_1\rangle_0\langle v_i\rangle_{1I} + \langle s_1\rangle_{1I}\langle v_i\rangle_0) - \frac{1}{L_t}(\langle s_2\rangle_0\langle v_0\rangle_{1I} + \langle s_2\rangle_{1I}\langle v_0\rangle_0 = -\frac{R_t}{L_t}(it_{1I}) - w_S(it_{1R}) + \frac{1}{L_t}\frac{-2\cos d\pi}{\pi}(v_i) - \frac{1}{L_t}\frac{-2\sin d\pi}{\pi}(V_{00}) \quad (21)$$

$$\frac{d\langle v_0\rangle_0}{dt} = -\frac{1}{C_0}\langle i_N\rangle_0 - \frac{1}{RC_0}\langle v_0\rangle_0 + \frac{1}{C_0}\langle s_2\rangle_0\langle it\rangle_0 + \frac{2}{C_0}\langle s_2\rangle_{1R}\langle it\rangle_{1R} + \frac{2}{C_0}\langle s_2\rangle_{1I}\langle it\rangle_{1I} = -\frac{i_N}{C_0}\langle i_N\rangle_0 - \frac{V_{00}}{RC_0} + 0 + \frac{2}{C_0}\frac{-2\sin d\pi}{\pi}(it_{1R}) + \frac{2}{C_0}\frac{-2\cos d\pi}{\pi}(it_{1I}) \quad (22)$$

5. Simulation Results

The EVFCS with front end VSC and DAB converter is simulated in MATLAB/Simulink. The VSC is rated for 15kVA, each DAB is rated for 8kVA. The VSC controllers are tuned to regulate the common DC bus voltage to 800V. The EV battery stack connected to the output of DAB is charged in Constant Current mode. The current references as dictated by the user set references are tracked by the PI controllers of DAB converter. The DAB converters are switched at a high switching frequency of 100kHz. Figure 3(a) shows the waveforms of the AC voltages and AC currents. Figure 3(b) shows the DC bus voltage nd DC bus current. It can be seen that the DC bus voltage is maintained constant at all operating points regardless of the battery current reference changes. During the battery current reference change, there is a small oscillation and it is regulated to the constant value. The DC bus current varies as the battery current drawn is varied. The battery voltage and battery current are shown in fig 4. It can be seen that the battery voltage is constant and the battery current is tracked around the reference point. The battery current reference is indicated by the blue waveform and the battery current measured with the sensor is indicated by the orange waveform. The outer phase shift (d) is shown in fig 5(a) and the primary, secondary voltages of the DAB transformer are shown in fig 5(b).

Power System Technology
ISSN:1000-3673

Received: 16-06-2025 *Revised: 05-07-2025* *Accepted: 20-08-2025*

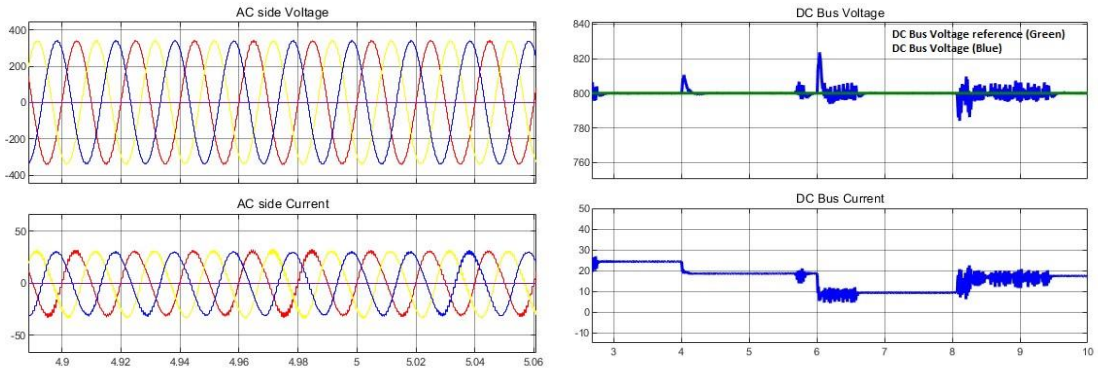

(a) (b)

Figure 3: (a) Simulation Results of the AC grid Voltage and Current and (b) VSC DC bus Voltage and Current

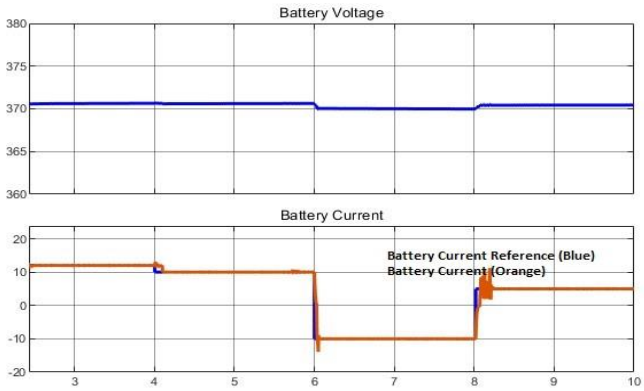

Figure 4: Simulation Results of the Battery Voltage and Battery Current

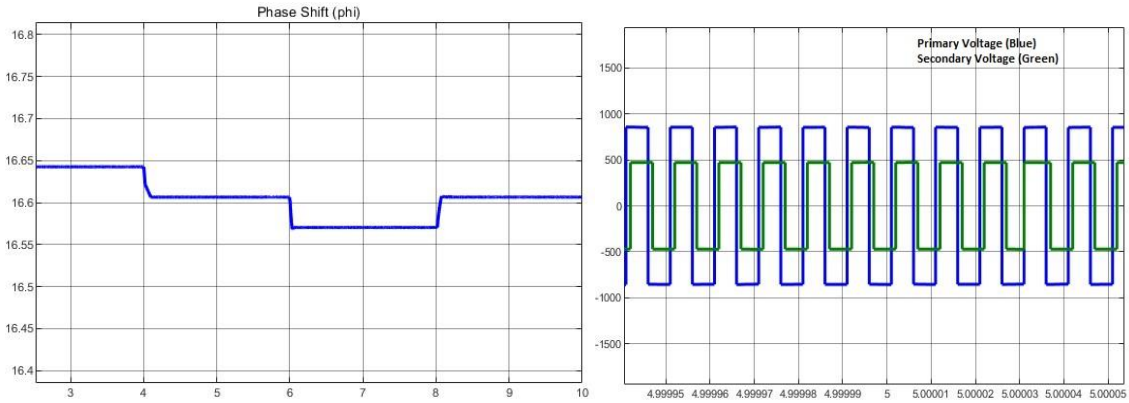

(a) (b)

Figure 5: (a) Simulation Results of the Phase Shift in DAB converter and (b) Primary and Secondary side voltages of the DAB Transformer

Power System Technology
ISSN:1000-3673
Received: 16-06-2025 Revised: 05-07-2025 Accepted: 20-08-2025

Figure 6 shows the switch voltage and switch current along with the gating signal. It can be seen that during turn on Zero Current Switching (ZCS) occurs and during turn off Zero Voltage Switching (ZVS) occurs.

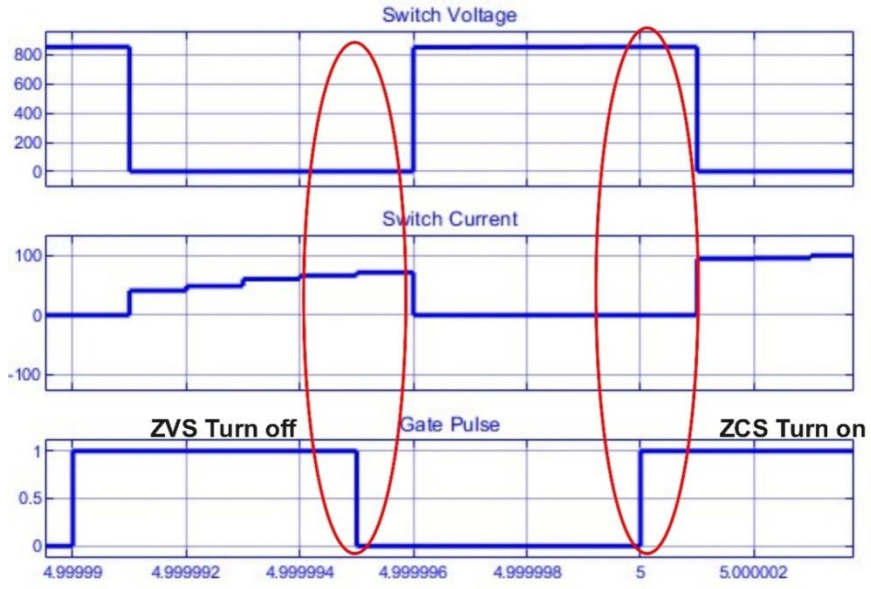

Figure 6: Simulation results showing ZVS and ZCS of switch S1

6. Experimental Results

In order to verify the proposed control scheme, the experimental validations are carried out on OP4610. The circuit parameters of the system is given in Table 1. The control scheme is implemented in OP4610 (Real Time Digital Simulator).

Table 1: System Parameters

S.No	Parameter	Value
1	AC Grid Voltage	415V, 3Ø
2	AC Grid Frequency	50Hz
3	Common DC Bus Voltage	800 V
4	Switching Frequency of VSC	5kHz
5	HF Transformer turns ratio, n	0.45
6	Switching Frequency of DAB	100kHz
7	DAB Output Voltage	360 V

Power System Technology
ISSN:1000-3673
Received: 16-06-2025 Revised: 05-07-2025 Accepted: 20-08-2025

Figure 7 shows the experimental waveforms obtained from the DSO. The EVFCS is simulated in OP4610. The DC bus voltage and DC bus current is shown in fig 7(a). The AC grid voltages are shown in fig 7(b). The battery current and the battery voltage are shown in fig 7(c). The switching waveforms are shown in fig 7(d).

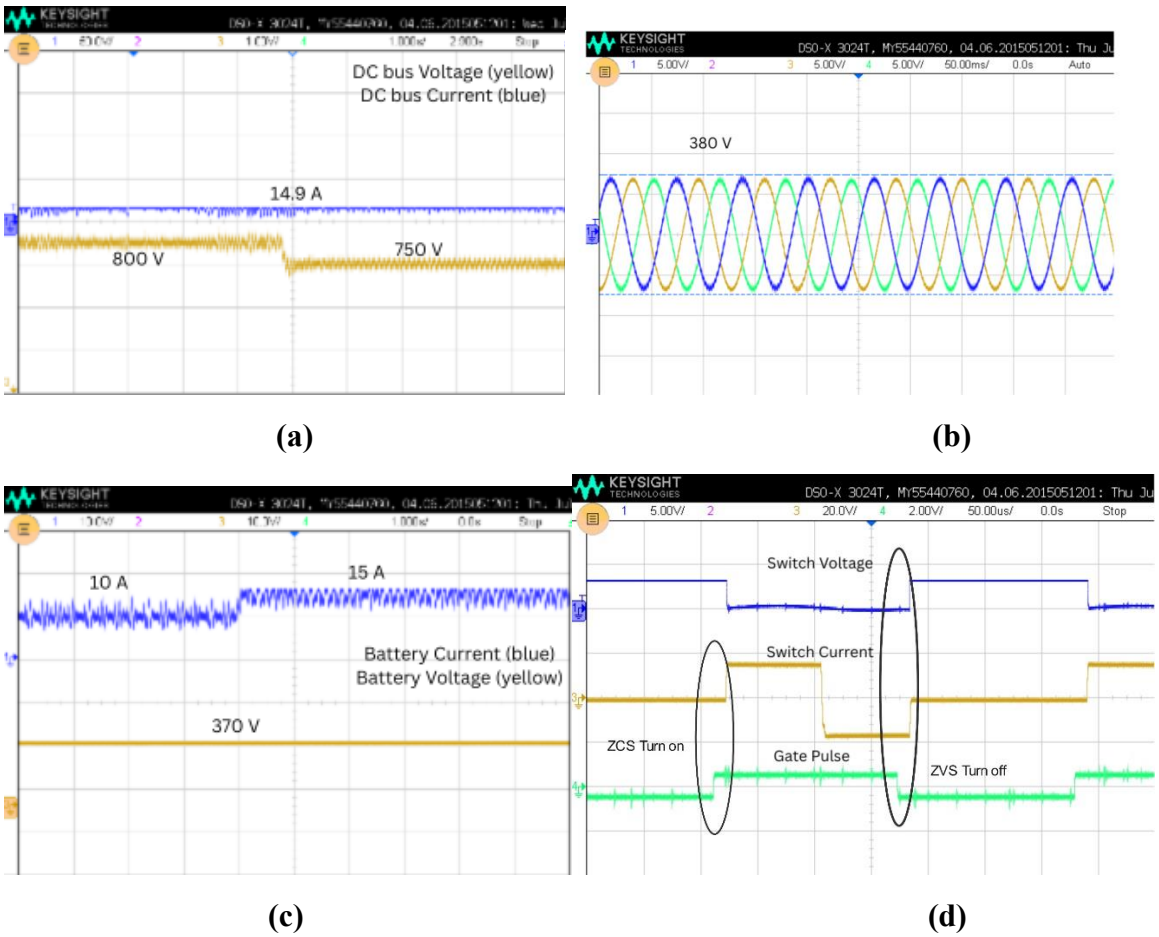

Figure 7:Experimental Results (a) VSC DC bus Voltage and Current, (b) AC Grid Voltages, (c) Battery Current and Battery Voltage and (d) Switch Voltage, Switch Current and Gate Pulse

7. Conclusion

The EVFCS with the improved soft switching region is simulated in MATLAB/Simulink and the results are verified with the experiment results. The front end VSC controllers are designed to maintain a stiff DC bus voltage of 800V and draw very minimal reactive power by setting the q axis current reference as 0. The DAB converter is designed to charge the battery at CC mode by the action of cascaded PI controllers regulating the outer phase shift and inner phase shift. The switching waveforms shows ZCS turn on and ZVS turn off.

Power System Technology
ISSN:1000-3673

Received: 16-06-2025 *Revised: 05-07-2025* *Accepted: 20-08-2025*

Control prototyping is done with OP4610. It can be found that with the improved TPS scheme the soft switching is achieved in the wide operating range.

Acknowledgement

This work was supported by SPD MHRD RUSA2.0

Refrences

[1] "Global EV outlook 2021," International Energy Agency,2021. [Online] Available : https://iea.blob.core.windows.net/assets/ed5f4484-f556-4110-8c5c-4ede8bcba637 /GlobalEVOutlook2021.pdf

[2] Samaras C, Meisterling K. Life cycle assessment of greenhouse gas emissions from plug-in hybrid vehicles: implications for policy. Environ Sci Technol. 2008 May 1;42(9):3170-6. doi: 10.1021/es702178s. PMID: 18522090

[3] M. Safayatullah, M. T. Elrais, S. Ghosh, R. Rezaii and I. Batarseh, "A Comprehensive Review of Power Converter Topologies and Control Methods for Electric Vehicle Fast Charging Applications," in IEEE Access, vol. 10, pp. 40753-40793, 2022, doi: 10.1109/ACCESS.2022.3166935.

[4] H. Heydari-doostabad and T. O'Donnell, "A Wide-Range High-Voltage-Gain Bidirectional DC–DC Converter for V2G and G2V Hybrid EV Charger," in IEEE Transactions on Industrial Electronics, vol. 69, no. 5, pp. 4718-4729, May 2022, doi: 10.1109/TIE.2021.3084181.

[5] U. Sharma and B. Singh, "A Generalised Double Integral Sliding Mode Control for Bidirectional Charger of Light Electric Vehicle," 2019 IEEE International Conference on Environment and Electrical Engineering and 2019 IEEE Industrial and Commercial Power Systems Europe (EEEIC / I&CPS Europe), 2019, pp. 1-6, doi: 10.1109/EEEIC.2019.8783407.

[6] V. K. Kanakesh, D. B. Yelaverthi, A. Ghoshal, A. K. Rathore and R. Mahanty, "Analysis and Implementation of Closed-Loop Control of Electrolytic Capacitor-Less Six-Pulse DC-Link Bidirectional Three-Phase Grid-Tied Inverter," in IEEE Transactions on Industry Applications, vol. 54, no. 1, pp. 539-550, Jan.-Feb. 2018, doi: 10.1109/TIA.2017.2757438.

[7] S. Kim and F. Kang, "Multifunctional Onboard Battery Charger for Plug-in Electric Vehicles," IEEE Trans. Ind. Electron., vol. 62, no. 6, pp. 3460-3472, Jun. 2015.

[8] A. M. Elrajoubi, S. S. Ang and K. George, "Design and analysis of a new GaN-based AC/DC converter for battery charging application," IEEE Trans. Ind. Appl., vol. 55, no. 4, pp. 4044-4052, Jul. 2019.

Power System Technology
ISSN:1000-3673

Received: 16-06-2025 *Revised: 05-07-2025* *Accepted: 20-08-2025*

[9] U. R. Prasanna, A. K. Singh and K. Rajashekara, “Novel Bidirectional Single-phase Single-Stage Isolated AC–DC Converter With PFC for Charging of Electric Vehicles,” IEEE Trans. Transport Elec., vol. 3, no. 3, pp. 536- 544, Sept. 2017.

[10] S. V. Anbuselvi, R. Brinda, B. Sripriya and R. P. K. Devi, "Performance Analysis of 2.4KW CLLC Resonant Dual Active Bridge Converter with Different Phase Shift Modulation Techniques for EV Charging Applications," 2023 IEEE Transportation Electrification Conference and Expo, Asia-Pacific (ITEC Asia-Pacific), Chiang Mai, Thailand, 2023, pp. 1-8, doi: 10.1109/ITECAsia-Pacific59272.2023.10372247.

[11] M. N. Kheraluwala, R. W. Gascoigne, D. M. Divan and E. D. Baumann, "Performance characterization of a high-power dual active bridge DC-to-DC converter," in IEEE Transactions on Industry Applications, vol. 28, no. 6, pp. 1294-1301, Nov.-Dec. 1992, doi: 10.1109/28.175280.

[12] N. Hou and Y. W. Li, "Overview and Comparison of Modulation and Control Strategies for a Nonresonant Single-Phase Dual-Active-Bridge DC–DC Converter," in IEEE Transactions on Power Electronics, vol. 35, no. 3, pp. 3148-3172, March 2020, doi: 10.1109/TPEL.2019.2927930.

[13] F. Krismer and J. W. Kolar, “Efficiency-optimized high-current dualactivebridge converter for automotive applications,” Industrial Electronics,IEEE Transactions on, vol. 59, no. 7, pp. 2745–2760, 2012.

[14] Parikshith Channegowda, Vinod John, “Filter Optimization for Grid Interactive Voltage Source Inverter”, in IEEE Transactions on Industrial Electronics, vol. 57, no. 12, 2010

[15] Nargunadevi TS, Anbuselvi SV, Kumudini Devi RP, “Small Signal Stability based Controller Tuning for Enhanced LVRT Performance of VSC-HVDC Transmission System”, Power System Technology, vol. 49, no.2, pp. 394-415, 2025

[16] H. Qin and J. W. Kimball, "Generalized Average Modeling of Dual Active Bridge DC–DC Converter," in IEEE Transactions on Power Electronics, vol. 27, no. 4, pp. 2078-2084, April 2012, doi: 10.1109/TPEL.2011.2165734.